The EMBO Journal Vol. 21 No. 12 pp. 2923–2935, 2002

Shigella deliver an effector protein to trigger host microtubule destabilization, which promotes Rac1 activity and efficient bacterial internalization

Sei Yoshida[1,2], Eisaku Katayama[3], Asaomi Kuwae[1], Hitomi Mimuro[1], Toshihiko Suzuki[1,2] and Chihiro Sasakawa[1,4]

[1]Department of Microbiology and Immunology and [3]Department of Basic Medical Sciences, Institute of Medical Science, University of Tokyo, 4-6-1, Shirokanedai, Minato-Ku, Tokyo 108-8639 and [2]PRESTO, Japan Science and Technology Corporation (JST), Japan

[4]Corresponding author
e-mail: sasakawa@ims.u-tokyo.ac.jp

Shigella **deliver a subset of effectors into the host cell via the type III secretion system, that stimulate host cell signal pathways to modulate the actin dynamics required for invasion of epithelial cells. Here we show that one of the *Shigella* effectors, called VirA, can interact with tubulin to promote microtubule (MT) destabilization, and elicit protrusions of membrane ruffling. Under *in vitro* conditions, VirA inhibited polymerization of tubulin and stimulated MT destabilization. Upon microinjection of VirA into HeLa cells, a localized membrane ruffling was induced rapidly. Overexpression of VirA in host cells caused MT destruction and protruding membrane ruffles which were absent when VirA was co-expressed with a dominant-negative Rac1 mutant. Indeed, *Shigella* but not the *virA* mutant stimulated Rac1, including the formation of membrane ruffles in infected cells. Importantly, the MT structure beneath the protruding ruffling was destroyed. Furthermore, drug-induced MT growth in HeLa cells greatly enhanced the *Shigella* entry. These results indicate that VirA is a novel type of bacterial effector capable of inducing membrane ruffling through the stimulation of MT destabilization.**

Keywords: membrane ruffling/microtubule/*Shigella* invasion/VirA

Introduction

Many bacterial pathogens can direct their own internalization into non-phagocytic cells such as epithelial cells. This bacterial ability is important for the infection process, since bacterial internalization into epithelial cells results in either colonization therein or translocation across the mucosal barrier, and, in some cases, the pathogen sequesters itself within an infected organ or gains further access to deeper tissues. Invasive bacteria use various mechanisms to enter host cells and, based on these, they are categorized into two major classes; those expressing a microbial ligand that interacts with a host cell receptor, and those for which entry is mediated by delivery of bacterial proteins, called effectors, into the host cells to trigger profound membrane ruffling and macropinocytosis (Isberg and Tran Van Nhieu, 1994; Ireton and Cossart, 1998). The former type of invasion represented by *Yersinia pseudotuberculosis* (Isberg, 1991; Isberg and Tran Van Nhieu, 1994) or *Listeria monocytogenes* (Cossart and Lecuit, 1998; Ireton and Cossart, 1998) is mediated by a zipper-like mechanism. In this case, the bacterial internalization event is limited to its own uptake by the host cells. The latter class of invasion event represented by *Shigella flexneri* or *Salmonella typhimurium* allows uptake of other particles together with the invasive pathogens (Francis *et al*., 1993; Sansonetti, 1999; Bourdet-Sicard *et al*., 2000; Galán and Zhou, 2000). Despite these differences, invasive bacteria can remodel the host cell surface in a variety of ways, such as by stimulating Rho GTPases, protein tyrosine phosphorylation or lipid metabolism, and these events eventually lead to a rearrangement of the actin dynamics in host cells. In addition to the involvement of actin, in some cases cytoskeletal microtubules (MTs) also seem to be involved in the bacterial entry (Finlay and Falkow, 1997). Although the mechanisms underlying the modulation of MT dynamics as directed by pathogens are still poorly understood, alterations of MT dynamics have been implicated in the entry of various pathogenic bacteria such as *Actinobacillus actinomycetemcomitans* (Meyer *et al*., 1999), *Campylobacter jejuni* (Oelschlaeger *et al*., 1993) and *L.monocytogenes* (Kuhn, 1998).

The invasiveness of *Shigella* is an essential pathogenic feature of bacillary dysentery, since bacterial entry into and colonization within the colonic epithelial cells, including the subsequent cell-to-cell spreading, are prerequisites for the illness. Although the precise mechanisms underlying the invasive process of *Shigella* are still to be defined, the bacterial capability to trigger a profound rearrangement in the actin cytoskeleton at the point of bacterial contact with the host cell is crucial for invasion of epithelial cells, because this leads to the formation of large-scale membrane ruffling and macropinocytosis (Bourdet-Sicard *et al*., 2000). The delivery of effector proteins such as IpaA, IpaB, IpaC, IpaD, IpgD and VirA through the type III protein secretion system from *Shigella* into and onto host epithelial cells is a prerequisite for triggering such cellular responses (Sansonetti, 1999; Bourdet-Sicard *et al*., 2000). Although the precise role of each effector protein is still to be elucidated, recent studies have indicated that some of the effector molecules delivered, such as IpaA, IpaB, IpaC and IpaD, can modulate the host cell actin dynamics in various ways, including the signal transduction pathways required for bacterial invasion. The IpaA protein delivered into host cells binds vinculin, a component of focal adhesion, and the resulting IpaA–vinculin complex together with F-actin promotes depolymerization of actin filaments, which is

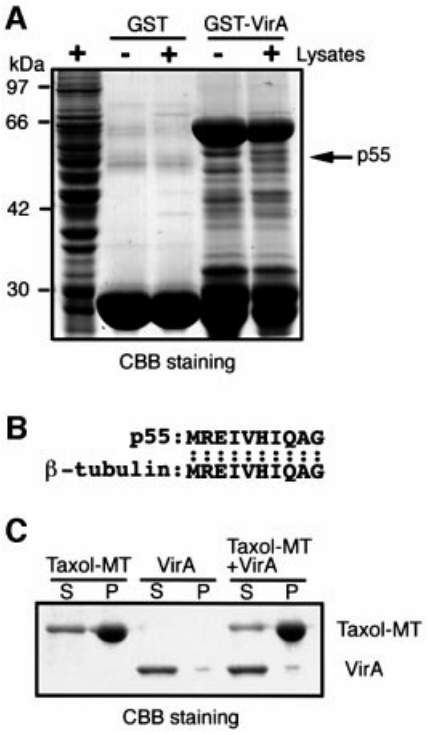

Fig. 1. Interaction of VirA with tubulin dimers *in vitro*. (**A**) The interaction of VirA with a 55 kDa protein (p55, arrow) in bovine brain lysates was examined by a GST pull-down assay. Proteins bound to GST or GST–VirA beads were separated by SDS–PAGE on 10% gels before being stained with Coomassie Brilliant Blue (CBB). (**B**) N-terminal amino acid sequence analysis of the 55 kDa protein (p55) showed that it was identical to the N-terminal 10 amino acids of bovine β-tubulin. (**C**) *In vitro* binding assay of taxol-MT and VirA. A 10 µl aliquot of 35 µM taxol-MT and 30 µl of 12 µM purified VirA (test; Taxol-MT + VirA) or 30 µl of PM buffer (control 1; Taxol-MT) were mixed gently and incubated for 10 min at room temperature. At the same time, 10 µl of PM-4M buffer containing 35 µM taxol and 30 µl of 12 µM purified VirA were also mixed gently and incubated for 10 min at room temperature (control 2; VirA). Each mixture was layered onto a 40 µl cushion of 60% glycerol containing 10 µM taxol, and sedimentated for 10 min at 100 000 *g* at room temperature. After the centrifugation, the supernatants (total: 80 µl) were added to 20 µl of 5× SDS sample buffer, while the pellets was dissolved into 100 µl of 1× SDS sample buffer. For SDS–PAGE analysis, 9.5 µl of each sample were run on the 10% gel, and the proteins were stained with CBB. Little VirA was pelleted with taxol-MT. P, pellet; S, supernatant.

thought to be required for the modification of *Shigella*-induced membrane protrusions (Tran Van Nhieu *et al*., 1997; Bourdet-Sicard *et al*., 1999). The secreted IpaC is integrated into the host plasma membrane and can modulate actin dynamics, since the formation of filopodia and lamellipodia is induced when purified IpaC protein is added to permeabilized Swiss 3T3 cells or when an *ipaC* clone is transfected into HeLa cells (Tran Van Nhieu *et al*., 1999; Kuwae *et al*., 2001). IpaC-induced membrane protrusions can be inhibited by a dominant-negative form of Cdc42, while a dominant-negative form of Rac1 inhibits the formation of lamellipodia, suggesting that IpaC induces activation of Cdc42 which, in turn, may cause the activation of Rac1 (Tran Van Nhieu, 1999). Other studies have also indicated that RhoA, Rac1 and Cdc42 control the entry of *Shigella* into epithelial cells, since their dominant-negative forms caused a significant reduction in the efficiency of *Shigella* invasion into these mutant host cells (Watarai *et al*., 1997; Mounier *et al*., 1999).

We previously identified the *virA* gene of *S.flexneri* as being required for the efficient entry of bacteria into epithelial cells (Uchiya *et al*., 1995). In that study, we showed that the *virA* mutant of *S.flexneri* had decreased invasiveness, with a level of only 20–30% that of the wild-type, as determined by the gentamicin killing assay. In addition, we also found that the secretion of VirA into the culture medium is dependent on the type III secretion system. Nevertheless, the *virA* mutant still possessed the wild-type level of contact haemolytic activity, an ability of *Shigella* to lyse red blood cells by forming IpaB–IpaC pores in the host plasma membrane, and which is required for delivery of the effector proteins into the host cells (Blocker *et al*., 1999). Therefore, these studies have strongly suggested that the role of VirA in the invasion of epithelial cells is Ipa independent, and that VirA acts as an effector protein in modulating the host function during *Shigella* invasion (Uchiya *et al*., 1995).

In this context, we wished to elucidate the function of VirA as an effector molecule during *S.flexneri* invasion of epithelial cells. The data presented in this study provide evidence for the first time indicating that VirA is a novel type of bacterial effector, which induces lamellipodia and efficient bacterial internalization into epithelial cells through the stimulation of MT destabilization.

Results

VirA interacts with α/β-tubulin heterodimers

To investigate the interactions between VirA and any potential host factor proteins during *Shigella* invasion of epithelial cells, host proteins were used in a GST–VirA pull-down assay with bovine brain extract (Miki *et al*., 1994). Analysis of the precipitated proteins by SDS–PAGE showed that a 55 kDa protein (p55) was associated with GST–VirA but not GST alone (Figure 1A). The N-terminal amino acid sequence of p55 is identical to the N-terminal 10 amino acids of β-tubulin (Figure 1B). Immunoblotting of p55 with an anti-β-tubulin antibody confirmed that the protein bound by GST–VirA was β-tubulin. In the immunoblotting, p55 reacted with the anti-α-tubulin antibody (data not shown), suggesting that VirA associates with tubulin heterodimers. The ability of GST–VirA to interact with tubulin dimers was also reproducible in other GST–VirA pull-down assays using the lysates from HeLa, Swiss 3T3 and COS-7 cells (data not shown). Next, we investigated whether VirA could bind to polymerized tubulin (microtubule: MT) by preparing taxol-stabilized MT (taxol-MT). Taxol-MT was prepared as described in Materials and methods. For the assay, 10 µl of 35 µM taxol-MT and 30 µl of 12 µM purified VirA (test) or 30 µl of PM buffer (control 1) were mixed gently and incubated for 10 min at room temperature. At the same time, 10 µl of PM-4M buffer containing 35 µM taxol and 30 µl of 12 µM purified VirA were also mixed gently and incubated for 10 min at room temperature (control 2). The mixture was then layered onto 40 µl of 60% glycerol and sedimented for 10 min at 100 000 *g* at 4°C. The supernatant and pellet were collected and mixed with SDS sample buffer for the SDS–PAGE. As shown in

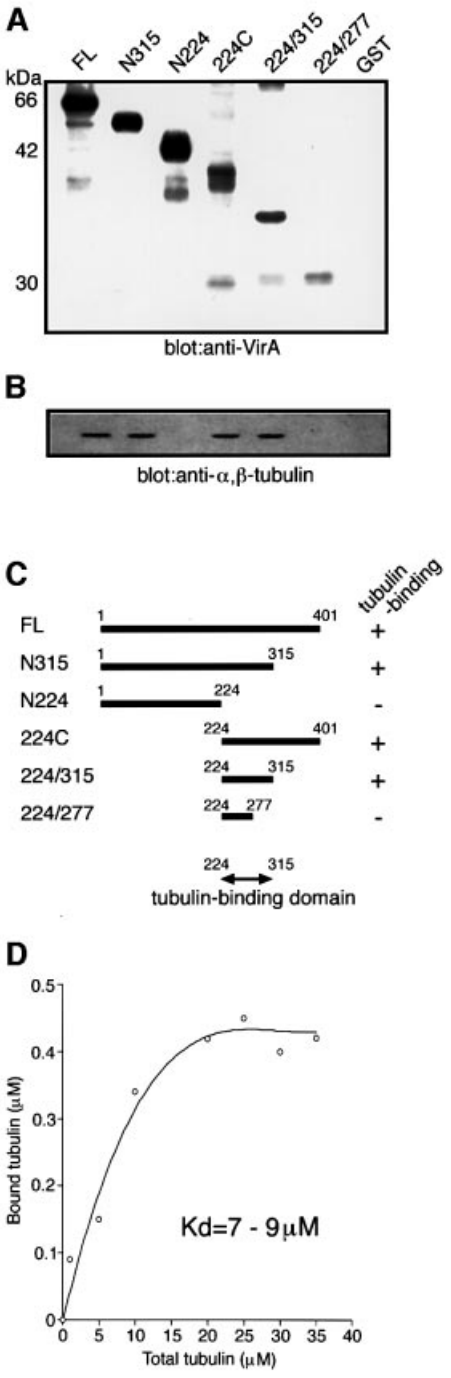

Fig. 2. *In vitro* binding assay of tubulin and VirA. (**A**) GST–VirA variants were fractionated by SDS–PAGE and western blotted with anti-VirA-FL. (**B**) *In vitro* association of tubulin dimers with GST–VirA variants immobilized on glutathione–Sepharose beads. Purified tubulin was incubated with GST–VirA variants immobilized on glutathione–Sepharose beads for 1 h at 4°C. The beads subsequently were washed, subjected to SDS–PAGE and then immunoblotted with a mixture of anti-α- and anti-β-tubulin antibodies. (**C**) Schematic representation of the constructs for GST–VirA fusion proteins and a summary of the tubulin-binding assays. A diagram indicating the extent of the tubulin-binding domain is shown at the bottom of the figure. (**D**) Various concentrations of tubulin (0, 1, 5, 10, 20, 25, 30 and 35 μM) were incubated with VirA beads (1 μM) for 1 h at 4°C. The beads were then subjected to SDS–PAGE and visualized by Coomassie Brilliant Blue staining (CBB). The amount of bound tubulin as well as of total tubulin was determined by densitometric analysis of the CBB-stained gels.

Figure 1C, very little VirA was pelleted with taxol-MT, suggesting that VirA is unable to bind MTs.

To confirm further the ability of VirA to bind tubulin dimers and identify the domain involved in the binding, we constructed the truncated VirA proteins, N315 (N-terminal 315 residues), N224 (N-terminal 224 residues), 224C (C-terminal 178 residues), 224/315 (residues 224–315) and 224/277 (residues 224–277) (Figure 2A and C). The VirA derivatives together with the full-length VirA (401 residues, FL) or GST alone were immobilized by glutathione–Sepharose-4B beads and an *in vitro* binding assay was performed with tubulin purified from bovine brain (Williams and Lee, 1982). Each set of beads was incubated with equivalent molar amounts of purified tubulin for 1 h at 4°C. After centrifugation, the amounts of bound tubulin in the pellets were measured by immunoblotting with anti-α- and β-tubulin antibodies. As seen in Figure 2B, FL, N315, 224C and 224/315 all precipitated tubulin, but N224, 224/277 and GST alone did not. These results suggest that the residues from 224 to 315 of VirA are involved in the interaction with tubulin (Figure 2C). To assess the affinity of the VirA–tubulin interaction, we measured the binding of purified tubulin to VirA (1 μM)-bound beads in the presence of various tubulin concentrations (0–35 μM). As shown in Figure 2D, the deduced K_d value was ~8 μM, and the binding stoichiometry was estimated to be ~1:2 (tubulin dimers: GST–VirA). Under the same conditions, GST–224/277 did not bind tubulin (data not shown). Thus, once again the results strongly suggest that VirA has the ability to bind tubulin heterodimers.

VirA disassembles stable microtubules in vitro

The MT dynamics in mammalian cells have been shown to be modulated by MT-stabilizing and -destabilizing factors (Desai and Mitchison, 1997). Hence, we investigated whether VirA could affect MT stabilization or destabilization using twice-cycled MT proteins, which contained MAPs (microtubule-associated proteins, known as MT-stabilizing factors), prepared from bovine brain lysates (Williams and Lee, 1982), and VirA protein from GST–VirA (Figure 3A). Upon incubation in PM-1.3M buffer, the twice-cycled MT proteins were polymerized at 37°C (Figure 3B). The polymerized MTs (6 μM) in the presence or absence of VirA were monitored spectrophotometrically (A_{350}) at 37°C using temperature-controlled cuvettes. In the absence of VirA, the MTs depolymerized slightly after 30 min (Figure 3C, crosses). However, the addition of VirA (6 μM) resulted in an almost complete depolymerization of the MTs within 10 min (Figure 3C, filled triangles), and this effect was dose dependent (Figure 3C). The destabilization by VirA was comparable with its inhibitory effect on the assembly of tubulin. In fact, when VirA was added to the assay buffer containing pre-assembled MTs, VirA disrupted the polymerization of tubulin in a dose-dependent manner (Figure 3D). Under these conditions, little MT destabilization was observed with N224, a VirA-truncated mutant (Figures 3C and D, inset graphs).

To confirm further the effect of VirA on MT destabilization, X-rhodamine-labelled MTs were prepared as described in Materials and methods. A 3 μl aliquot of the X-rhodamine-MTs (3.5 mg/ml) was mixed with either

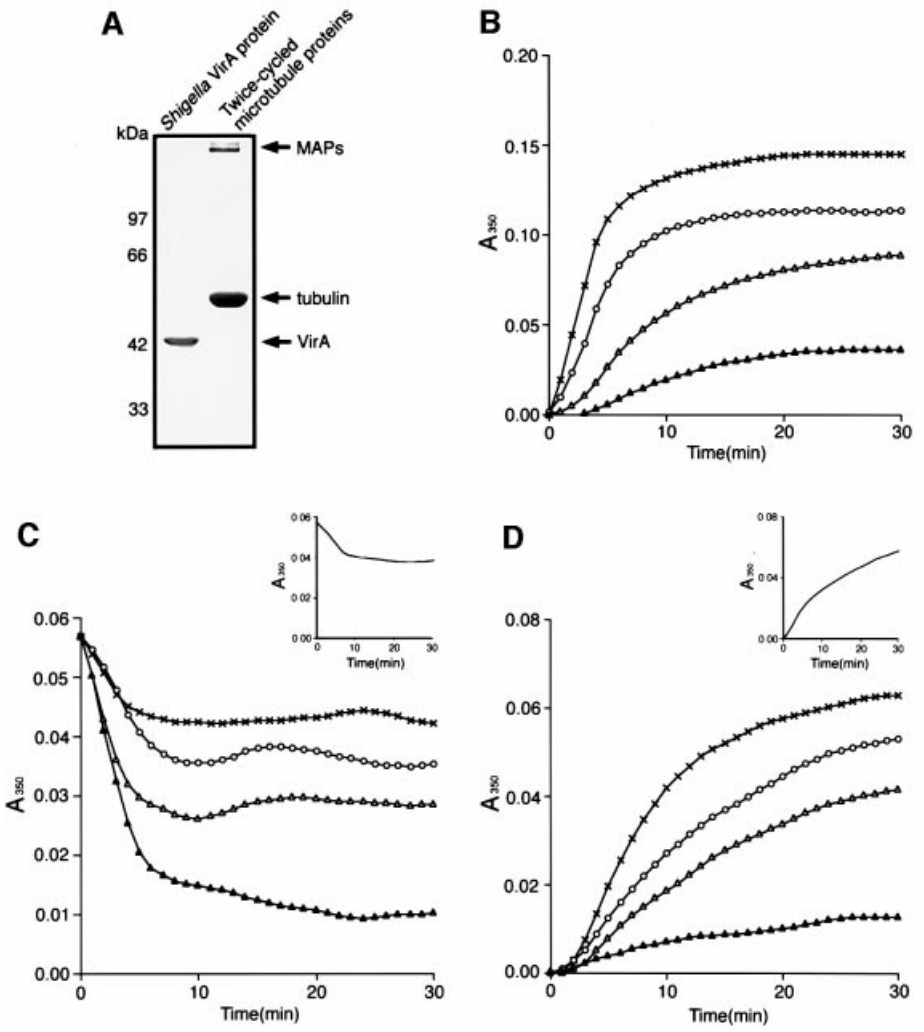

Fig. 3. VirA induces MT destabilization *in vitro*. (**A**) Purified VirA and twice-cycled MT proteins were separated by SDS–PAGE on 10% gels and then stained with Coomassie Blue. (**B**) Purified twice-cycled MT proteins in PM buffer (100 mM PIPES-NaOH pH 6.9, 2 mM EGTA, 1 mM $MgSO_4$, 2 mM DTT, 1 mM GTP) containing 1.3 M glycerol (PM-1.3M) were polymerized as measured spectrophotometrically (filled triangles, 7 μM; open triangles, 10 μM; open circles, 12 μM; crosses, 15 μM). (**C**) VirA induces MT destabilization. After polymerization, MTs (12 μM) were mixed with the same volume of either PM-1.3M buffer alone (crosses) or PM-1.3M buffer containing VirA (open circles, 3 μM; open traingles, 6 μM; filled triangles, 12 μM). Destabilization of MTs was monitored at A_{350} for 30 min. Under the same conditions, little MT destabilization was observed with 12 μM N224 (a VirA truncated mutant) (small graph). (**D**) VirA inhibits MT polymerization. Tubulin (9 μM) was polymerized without (crosses) and with VirA (open circles, 2.25 μM; open triangles, 4.5 μM; filled triangles, 9 μM). Under the same conditions, N224 (9 μM) barely inhibited MT polymerization (small graph).

1 μl of 1 mg/ml VirA or PM buffer alone. The samples were then diluted with 100 μl of PM-1.3M buffer, and immobilized on a glass coverslip, before being observed by confocal microscopy. As shown in Figure 4, the original MT structure was still intact after 30 min incubation in buffer alone (Buffer); however, in the presence of VirA, the structure of the MTs had almost disappeared after a 30 min incubation (+VirA). Under the same conditions, the MT structure was still intact with N224 (+N224) even after a 30 min incubation. The quantification of the mean MT length using random fields from the fluorescent MT experiment showed that the mean length for the control was 6.19 ± 0.54 μm at time 0 and 4.19 ± 0.45 μm after 30 min (Buffer, n = 20), while for +VirA it was 6.78 ± 0.72 μm at time 0 and 1.99 ± 0.27 μm after 30 min (+VirA, n = 20). Thus, the results further indicate that VirA has the ability to promote destabilization of the MTs.

VirA causes MT destabilization in vivo and membrane ruffling

To investigate further the effects of VirA on MT destabilization, we constructed COS-7 cells overexpressing VirA by transfecting the cells with pVirA-FL [encoding green fluorescent protein (GFP)–VirA], pVirA-N315 (encoding GFP–N315 VirA mutant) or pVirA-N224 (encoding GFP–N224 VirA mutant). COS-7 transfectants overexpressing full-length VirA showed changes in cell shape with a profusion of membrane ruffles around the periphery, but these effects were not observed with N315 (not shown), N224 or vector alone (Figure 5A). In COS-7 transfectants with pVirA-FL, the radiation pattern of the

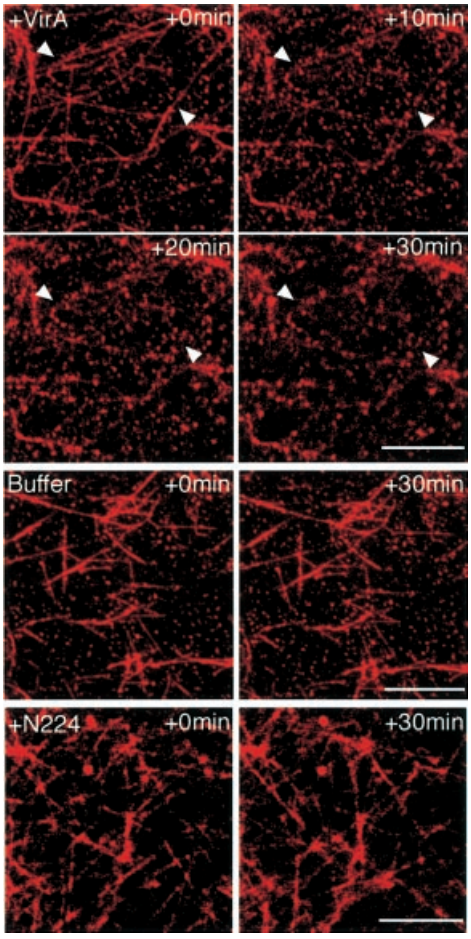

Fig. 4. X-rhodamine–tubulin assay. The structure of the X-rhodamine-MT almost completely disappeared when incubated with VirA for 30 min (arrowheads, +VirA), but it was still intact when incubated for 30 min with PM buffer alone (Buffer) or N224 (+N224). Bar, 10 μm.

MT networks was severely destroyed, and GFP–VirA was found associated with these altered MTs (Figure 5A, FL). In contrast, COS-7 transfectants with pVirA-N224 showed no significant changes in cell shape or the MT networks, and GFP–N224 was not co-localized with the MT networks (Figure 5A, N224). The rate of the appearance of ruffles around the periphery in COS-7 transfectants overexpressing VirA-FL was 3-fold higher than that of COS-7 transfectants overexpressing VirA-N315, VirA-N224 or vector alone (Figure 5A, graph). To eliminate the possibility that the observed VirA effects on cell shape in COS-7 cells might result from cytotoxity, HeLa cells overexpressing VirA-FL, VirA-N224 or the mock control were also examined. Only HeLa cells overexpressing VirA-FL were found to protrude the membrane ruffles with no changes in cell shape, and the GFP–VirA signal was co-localized with the MTs, the structure of which was destroyed in these ruffles (Figure 5B). Since previous studies indicated that destruction of the MT network in fibroblastic cells induced pharmacologically, such as by treatment with nocodazole, resulted in similar changes in cell shape, including the formation of membrane ruffling, to that displayed in COS-7 cells expressing VirA (Waterman-Storer *et al*., 1999), the above results indicate that *in vivo* the VirA itself has the ability to promote destruction of the MT network and induce membrane ruffling. To confirm the ability of VirA to induce membrane ruffles, we microinjected 300 μg/ml VirA or VirA mutant protein (VirA-N224) into mammalian cells, and the cellular responses were investigated by phase-contrast microscopy. Microinjection of VirA (Figure 5C) but not N224 (data not shown) into HeLa cells led to the formation of membrane ruffles at the point of injection as early as within 5 min. This ruffling continued for as long as 10 min after the injection, and the scale of the ruffles was maximal at 7–8 min (Figure 5C). Based on the results of this series of experiments, we concluded that VirA has the ability to induce MT destabilization and also stimulate membrane ruffling in mammalian cells.

VirA-induced membrane ruffling is dependent on Rac1 activity

MT dynamics have been implicated in the formation of membrane ruffles in various mammalian cells (Shelden and Wadsworth, 1993; Wadsworth and Bottaro, 1996; Waterman-Storer and Salmon, 1997; Mikhailov and Gundersen, 1998). Although the mechanism is still unknown, a recent study in fibroblasts has indicated that the MT growth induced upon removal of the MT-destabilizing drug nocodazole leads to the activation of Rac1, which in turn causes the induction of lamellipodial protrusions (Waterman-Storer *et al*., 1999). Thus, we presumed that in mammalian cells overexpressing VirA, the MT destabilization evoked by the effector protein would result in MT growth and activation of Rac1, thus leading to the formation of membrane ruffles. In order to test this idea, COS-7 cells were co-transfected with pVirA-FL and a plasmid encoding wild-type Rac1 or the dominant-negative form of Rac1 (N17Rac1), and the formation of membrane ruffles including their cell shape was investigated. COS-7 transfectants overexpressing both VirA-FL and wild-type Rac1 evoked membrane ruffling with the destruction of the MT networks (data not shown). In contrast, COS-7 transfectants overexpressing VirA and N17Rac1 had no membrane ruffling, even though the MT networks were destroyed (Figure 6). These results thus support our idea that the induction of membrane ruffling by VirA in mammalian cells results from the activation of Rac1, which is associated with the destruction of MT networks by VirA.

The host cytoskeletal architecture around invading Shigella

To establish the physiological relevance of the VirA activity displayed *in vitro* and *in vivo* to *Shigella* invasion of epithelial cells, we investigated the cytoskeletal architecture around invading bacteria using confocal microscopy. Upon invasion of HeLa cells with wild-type *Shigella*, the membrane protrusions appeared around the invading bacteria, and the local MT networks beneath the protruding ruffles underwent a remarkable destruction (Figure 7A). No such events were observed with the *virA* null mutant. To demonstrate this further, we investigated the architecture of the single MTs around the invading bacteria in a high resolution photograph. On wild-type *Shigella* that provoked local destruction of the MT structure, the VirA secreted from the bacteria as represented by the green immunofluorescence signal was

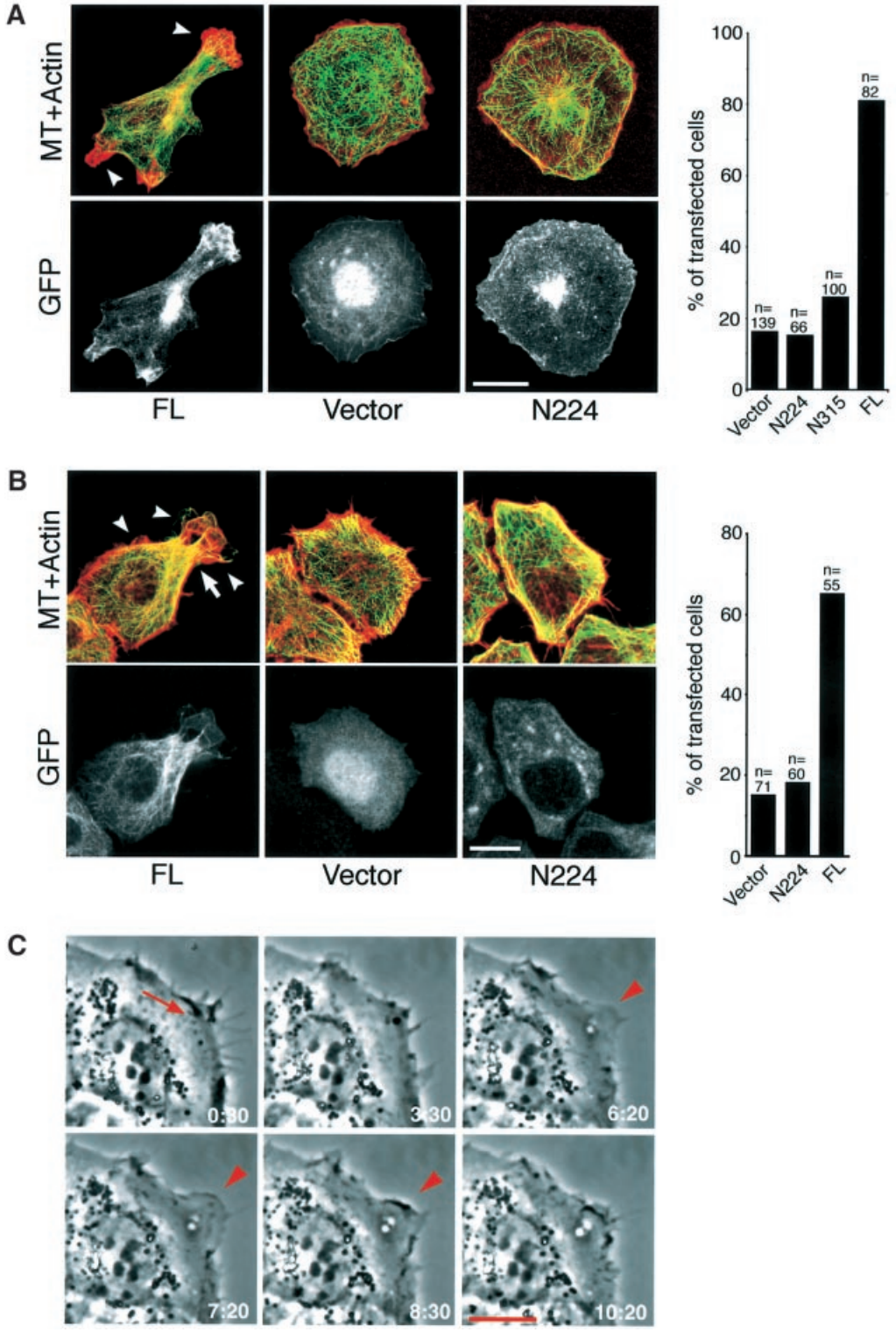

Fig. 5. VirA regulates MT stabilization and membrane ruffling. (**A**) COS-7 cells were transfected with plasmids encoding GFP–VirA (FL), GFP–VirA-N224 (N224) or vector alone (Vector). Actin (red in MT + Actin) and MT (green in MT + Actin) were visualized. The transfected cells were identified by GFP. COS-7 cells overexpressing VirA showed marked changes in cell shape with membrane ruffles around the periphery and, in addition, the MT networks, with which GFP–VirA was associated, were destabilized. Bar, 10 μm. The percentage of transfected COS-7 cells overexpressing GFP–VirA (FL), GFP–VirA-N315 (N315), GFP–VirA-N224 (N224) or GFP (Vector) showing marked changes in cell shape with membrane ruffles was calculated (graph). 'n' is the total number of cells examined in three independent experiments. (**B**) HeLa cells were transfected with the plasmid encoding GFP–VirA (FL), GFP–VirA-N224 (N224) or the vector alone (Vector). Actin (red in MT + Actin) and MT (green in MT + Actin) were visualized. The transfected cells were identified by GFP. HeLa cells overexpressing VirA showed membrane ruffles (arrowheads). The MT network associated with GFP–VirA beneath the ruffles had undergone alterations (arrow). Bar, 10 μm. The percentage of transfected HeLa cells overexpressing GFP–VirA (FL), GFP–VirA-N224 (N224) or GFP (Vector) showing membrane ruffles was calculated (graph). 'n' is the total number of cells examined in three independent experiments. (**C**) HeLa cells were microinjected (arrow) with VirA and observed by time-lapse video microscopy. Microinjection of VirA into HeLa cells led to membrane ruffling at the point of injection. The time elapsed after microinjection is shown in minutes:seconds. Arrowheads indicate membrane ruffles. Bar, 10 μm.

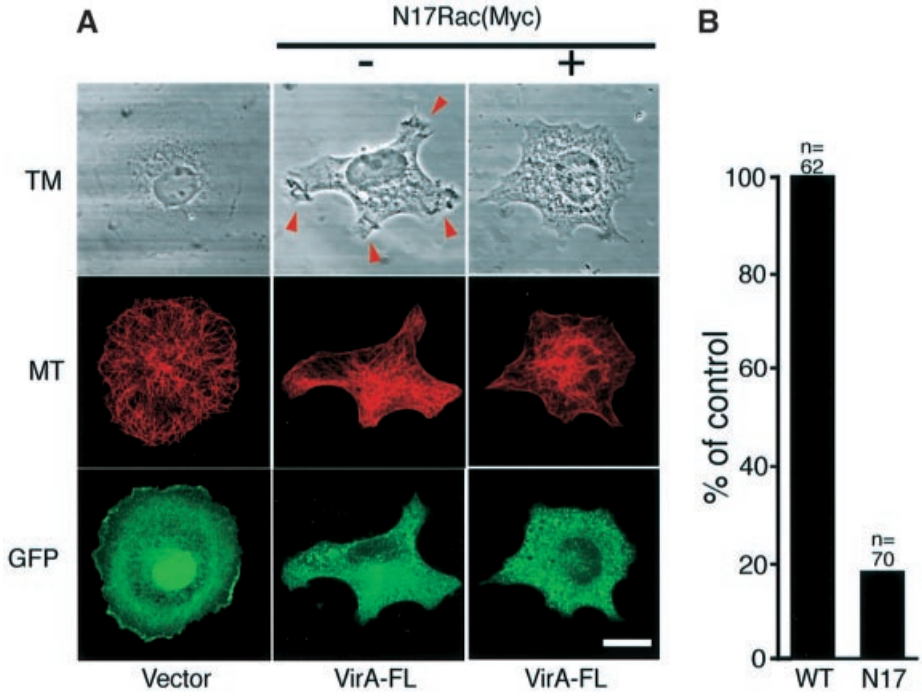

Fig. 6. VirA-induced membrane ruffling is dependent on Rac1 activity. (**A**) COS-7 cells were co-transfected with pVirA-FL and the plasmid encoding a Myc-tagged Rac1-T17N. After transfection for 18 h, the cells were stained with a mixture of anti-α- and anti-β-tubulin antibodies followed by Cy5-anti-mouse IgG antibody (MT, red) or GFP (green). The membrane ruffles (arrowheads) from the COS-7 cells overexpressing GFP–VirA disappeared on co-expression with Myc-tag N17Rac. TM: phase-contrast image. Bar, 10 μm. (**B**) Quantitative assay of membrane ruffles in COS-7 cells over-expressing both GFP–VirA and wild-type Rac (WT) or negative-form Rac (N17). Values represent the percentage relative to that of the control wild type (100%). 'n' is the total number of cells examined in three independent experiments.

detected mostly around the destroyed MTs (Figure 7B). Importantly, the ability of VirA to destroy the MT structure *in vivo* was observed further even after internalization of *Shigella* into the host cell cytoplasm, in which the local MT network surrounding the motile wild-type *Shigella* was also destroyed (data not shown).

MT growth in host cells promotes Shigella invasiveness

In agreement with the above results, the number of ruffles per *virA* mutant-infected cell was significantly lower (38%) than that with the wild-type *S.flexneri* (100%) (Figure 8Ab). It is noteworthy that the number of ruffles per cell infected with a *mxiA* mutant (defective in the type III secretion system) was low (4%) even compared with that of the *virA* mutant (38%), perhaps reflecting the contribution of other type III-mediated effectors such as IpaC to the promotion of membrane ruffling (Tran van Nhieu *et al*., 1999). Next, we examined the level of Rac1 activity in HeLa cells infected with *Shigella* by exploiting the Pak-binding domain (PBD), a specific target for the active form of Rac1 (Burbelo *et al*., 1995). Infection of HeLa cells with wild-type *Shigella* greatly enhanced the Rac1 activity, while the *virA* mutant did not (Figure 8Aa), indicating that VirA is involved in activation of Rac1 and the promotion of membrane ruffling.

To support further the notion that the MT destabilization induced by VirA *in vivo* contributed to the efficient invasion of *Shigella* into epithelial cells, we investigated the effect of MT growth induced pharmacologically on bacterial internalization. To induce MT growth, HeLa cells were pre-treated with the MT-destabilizing drug nocodazole and then washed, thus allowing for the induction of MT growth (Waterman-Storer *et al*., 1999). HeLa cells in which MT growth had been stimulated were then infected with wild-type *Shigella*, the *virA* mutant and the *virA* complement strain or the *mxiA* mutant, and their capacity to induce membrane ruffling was investigated. The numbers of membrane ruffles per bacterium associated with the HeLa cells were similar for the wild-type, the *virA* mutant and the *virA* complement strain (Figure 8B). Under these conditions, the number of internalized bacteria for each of the three strains as examined by the gentamicin killing assay was shown to be similar (data not shown). The results of this series of experiments strongly suggest that MT destabilization in host cells induced by VirA secreted from *Shigella* can provoke the formation of membrane ruffles, which stimulates the bacterial entry into the host cells.

Discussion

In this study, we have investigated the functional role of the *Shigella* effector, VirA, in promoting the invasion of epithelial cells. Our data indicate that VirA acts as an effector protein capable of inducing MT destabilization around the site of bacterial entry into the host cells. This ability would in turn lead to MT growth and the stimulation of Rac1 activity, thus evoking local membrane ruffling (Waterman-Storer *et al*., 1999; Wittmann and Waterman-Storer, 2001), required for efficient bacterial entry into the host cells. The observed VirA activity is in

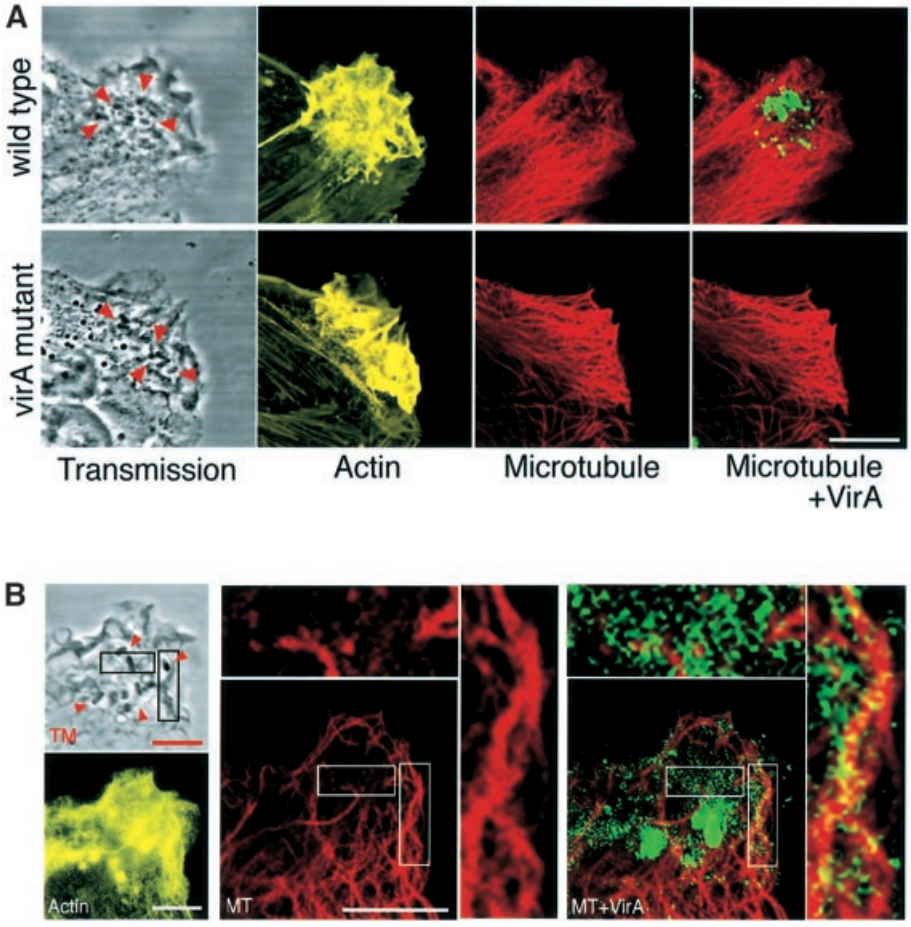

Fig. 7. Confocal microscopic observations of the invasion site for wild-type *Shigella* or the *virA* mutant. (**A**) HeLa cells were infected with wild-type or the *virA* null mutant. After a 15 min infection, the actin, tubulin and VirA were visualized by rhodamine–phalloidin (Actin, yellow), a mixture of anti-α- and anti-β-tubulin antibodies followed by Cy5-anti-mouse IgG antibody (MT, red) or the anti-VirA-FL antibody with an Alexa 488–anti-rabbit IgG antibody (VirA, green), respectively. Bar, 10 μm. Arrowheads indicate the bacteria. Upon attachment of the wild-type but not the *virA* mutant to HeLa cells, membrane protrusions appeared around the invading bacteria; at these points, the local MT networks beneath the protruding ruffles underwent a marked destruction. On wild-type *Shigella* that provoked local destruction of MT structure, secreted VirA from the bacteria was detected. (**B**) The local cytoskeletal architecture around the invading bacteria in a high resolution photograph. The actin, tubulin and VirA were visualized by rhodamine–phalloidin (Actin, yellow), a mixture of anti-α- and anti-β-tubulin antibodies followed by Cy5-anti-mouse IgG antibody (MT, red) or the anti-VirA-FL antibody with an Alexa 488–anti-rabbit IgG antibody (VirA, green), respectively. Bar, 10 μm. Arrowheads indicate the bacteria. The boxed portions of the MT network in (MT) and (MT + VirA) are shown enlarged. The VirA secreted from bacteria was detected mostly around the destroyed MTs.

agreement with our original report on VirA, where we found that the invasiveness of the *virA* mutant was significantly decreased as compared with that of the wild-type (Uchiya *et al*., 1995). This idea is deduced from the following results: (i) VirA binds α/β-tubulin heterodimers and destabilizes MTs both *in vitro* and *in vivo*; (ii) microinjection of VirA into HeLa cells leads to the formation of membrane ruffles at the point of injection; (iii) in mammalian cells overexpressing VirA, the MT networks are destroyed, and this is accompanied by the protrusion of lamellipodia; (iv) the membrane protrusions from COS-7 cells overexpressing VirA disappeared when VirA was co-expressed with a dominant-negative form of Rac1; (v) the local MT network at the *Shigella* invasive site undergoes destruction; and (vi) pharmacologically induced MT growth in host cells compensates for the reduced invasiveness of the *virA* mutant. Thus, all our results suggest that VirA is a unique effector with activity in mammalian cells unlike that of any other known bacterial effector proteins.

VirA interacts with MTs through direct binding to α/β-tubulin

Although the contribution of VirA to the bacterial invasion of epithelial cells has been controversial (Uchiya *et al*., 1995; Demers *et al*., 1998), the invasiveness of the *S.flexneri virA* mutant, N1945, as examined by the gentamicin killing assay was shown to be reduced to 20% of the wild-type level (Uchiya *et al*., 1995). Furthermore, since VirA has been shown to be secreted from *Shigella* into the medium via the type III secretion system under various conditions that stimulated the activity of this secretion system (Uchiya *et al*., 1995; Demers *et al*., 1998), we can assume that VirA plays an important role as an effector protein in stimulating uptake of bacteria by the host cells. Indeed, observations from immunofluorescence laser scanning microscopy showed that when *S.flexneri* was infecting HeLa cells, the VirA signal was detected in the host cells around the site of bacterial entry (Figure 7), suggesting that VirA is delivered from the bacteria into the host cells. Hence,

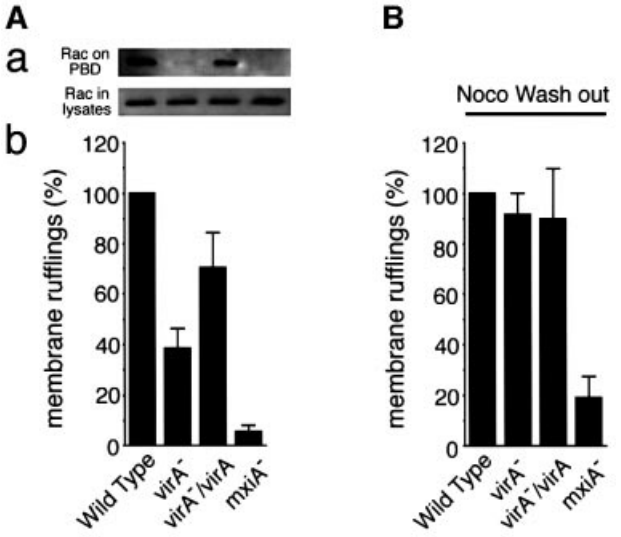

Fig. 8. MT growth in host cells promotes *Shigella* entry. (**A**) (a) Rac1 activation in HeLa cells upon *Shigella* invasion. Lysates of HeLa cells infected with wild-type *Shigella* (Wild Type), *virA* null mutant (virA$^-$), the *virA* mutant complemented with a cloned *virA* gene on a plasmid (virA$^-$/virA) or a *mxiA* mutant (deficient in type III secretion, mxiA$^-$) were incubated with the GST–PBD beads. The bound proteins were analysed by western blotting with an anti-Rac1 antibody. (b) Quantitative analysis of the number of ruffles per cells infected with wild-type, the *virA* mutant, the *virA* mutant complemented with a cloned *virA* gene on a plasmid or a *mxiA* mutant. The number of membrane ruffles per cell infected with the *virA* mutant was significantly lower (38%) than for the wild-type (100%). Values represent the percentage relative to that of the control wild-type (100%). The means and SEM are from three independent experiments. (**B**) Effect of MT growth on bacterial-induced membrane ruffles. To induce MT growth, HeLa cells were pre-treated with the MT-destabilizing drug, nocodazole. After the drug was washed out, the cells with MT growth thus stimulated were then infected by wild-type (Wild Type), the *virA* mutant (virA$^-$), the *virA* complement strain (virA$^-$/virA) or the *mxiA* mutant (mxiA$^-$) and investigated for their capacity to induce membrane ruffling. The number of membrane ruffles per bacterium associated with HeLa cells was similar for the wild-type, the *virA* mutant and the *virA* complement strain. Each value represents the percentage relative to that of the control wild-type (100%). The means and SEM are from three independent experiments.

the previous studies, taken together with our observations, led us to explore the target protein for VirA in the mammalian cells. A GST–VirA pull-down assay using bovine brain, together with HeLa, Swiss 3T3 or COS-7 cell extracts showed that VirA has the ability to interact with β-tubulin. Since the precipitated β-tubulin was always associated with α-tubulin, as shown by immunoblotting with anti-β- or anti-α-tubulin antibodies, it is likely that VirA interacts with tubulin heterodimers.

VirA has the ability to destabilize MTs

Our *in vitro* assay for the polymerization and depolymerization of twice-cycled MT proteins in the presence or absence of VirA suggests that VirA promotes MT destabilization. Indeed, in the presence of VirA, the polymerization of tubulin was inhibited in a concentration-dependent manner, while addition of VirA to MTs stimulated the depolymerization again in a concentration-dependent manner (Figure 3). The VirA activity was also demonstrated directly by observing the destabilized MTs using rhodamine-labelled MTs (Figure 4). Although the mechanisms underlying the MT destabilization by VirA still remain to be elucidated, based on our observations we speculate that VirA has the ability to induce MT destabilization.

It has been reported that many host proteins affect MT destabilization in cells (Desai and Mitchison, 1997). For example, cdc2 (Ookata *et al*., 1995) and MARK (Drewes *et al*., 1997) can induce phosphorylation of MAPs, which leads to a decrease in the MT-stabilizing capacity. Thus, the means by which the proteins induce destabilization of MTs is indirect. On the other hand, there are some other groups of proteins that can affect MT destabilization directly; these include MT-catastrophe factors such as XKCM1 (Desai *et al*., 1999) and MT-severing factors such as katanin (McNally and Vale, 1993), which are able to interact with MTs. In this regard, since VirA can bind tubulin dimers directly, but barely binds taxol-MT (Figure 1C), VirA would be categorized into some group other than the above. At present, two models might be considered to account for the VirA-induced MT destabilization. In the first model, VirA, like Op18 (stathmin) (Belmont and Mitchison, 1996), might somehow induce destabilization of the MTs through a mechanism in which the VirA-bound tubulin dimers might affect the MT stability. In fact, recent studies have indicated that Op18 has MT-sequestering activity which can decrease the critical concentration of free tubulin dimers to be polymerized in aqueous phase, thus promoting the MT destabilization (Cassimeris, 2002). Importantly, in the case of Op18, unlike VirA, it was hardly ever observed co-localized with MTs *in vivo* (Gavet *et al*., 1998). Our electron microscopic observation indicated that the purified monomeric VirA molecule in PM buffer at 4°C showed a two-globular like structure (unpublished data). Interestingly, when >10 μM VirA was incubated in PM buffer, the absorbance at 350 nm was significantly increased with an elevation in the incubation temperature (unpublished data). These observations are reminiscent of the behaviour of tubulin in PM buffer. It is thus intriguing to speculate that intracellular VirA could act as a competitor against tubulin dimers, which may in turn lead to local MT destabilization, as in the second model. Indeed, at physiological concentrations, MTs undergo both growing and shortening, termed dynamic instability, *in vitro* and *in vivo* (Desai and Mitchison, 1997). Under these conditions, the injection of VirA from the pathogen into the target host cells might result in it being integrated into the growing end instead of tubulin dimers, and this may cause a decrease in the MT stability. In any case, further experiments are clearly necessary to determine whether VirA binds tubulin dimers *in vivo* and how VirA destabilizes MTs in cells.

VirA stimulates Rac1 activity possibly through the induction of MT growth

Microinjection of VirA into HeLa cells rapidly induced membrane ruffling, albeit in a small scale (Figure 5C) as compared with that induced by *Shigella* invasion (Figure 7). Interestingly, in the case of fibroblastic cells such as NIH-3T3 and Swiss 3T3, microinjection of VirA can cause a rapid cellular retraction before protrusion of the membrane ruffles. For example, when VirA was injected into NIH-3T3 cells, a rapid cell retraction

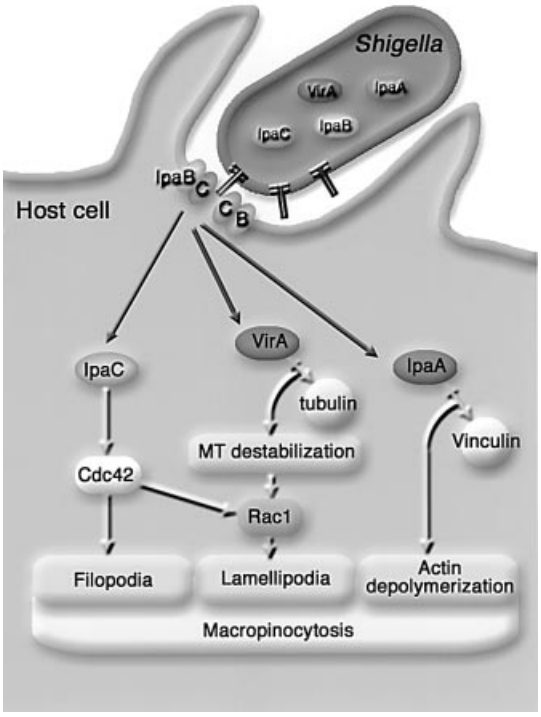

Fig. 9. Cytoskeletal rearrangements induced during *Shigella* invasion of epithelial cells. *Shigella* secretes the effector proteins, such as IpaB, IpaC, IpaA and VirA, into host cells. IpaB and IpaC are integrated into the host membrane, and IpaC modulates Cdc42-dependent filopodial formation which, in turn, may cause activation of Rac1 and lamellipodial formation. IpaA binds vinculin, and the resulting IpaA–vinculin complex promotes depolymerization of actin filaments, which is thought to be required for modulation of lamellipodial formation. VirA binds α/β-tubulin heterodimers and induces MT destabilization. VirA-induced MT destabilization would in turn lead to MT growth and stimulation of the Rac1 activity, and thus evoke the local membrane ruffling.

occurred within 5 min, and this continued for another 10 min. The retracted cells subsequently protruded membrane ruffles at the point of microinjection. The scale of ruffling was greater than that in HeLa cells and it was maximal at ~30 min after injection (unpublished data). Thus, these results strongly indicate that although the initial cellular response to VirA injection is somewhat different between epithelial cells and fibroblastic cells, VirA has the ability to induce local membrane ruffling in various types of mammalian cells.

Although the precise mechanisms underlying the induction of membrane ruffling by VirA remains to be elucidated, the local MT destabilization in cells evoked by VirA seems to be responsible. Interestingly, several studies have indicated that the MT's dynamic instability in mammalian cells can strongly affect the actin cytoskeletal dynamics during cell motility (Horwitz and Parsons, 1999; Ren *et al*., 1999; Waterman-Storer and Salmon, 1999). Importantly, a recent study indicated that MT growth can activate Rac1 and promote lamellipodial protrusion in fibroblasts (Waterman-Storer and Salmon, 1999; Waterman-Storer *et al*., 1999; Wittmann and Waterman-Storer, 2001). Although to date no cellular factor capable of directly inducing membrane ruffling through instability of MT dynamics has been reported, it has been indicated that MT growth can in turn induce local activation of Rac1, thus leading to the formation of membrane ruffles (Waterman-Storer *et al*., 1999). This would also be the case in the VirA-induced membrane ruffling as shown in Figure 5, since the extension of lamellipodia around the cells overexpressing VirA was greatly diminished when VirA was co-expressed with a dominant-negative Rac1, and where the GFP–VirA signals were associated with the altered MT networks (Figure 6). Although we cannot completely rule out the possibility of VirA directly activating Rac1, it is more likely that the VirA-induced MT destabilization contributes to the promotion of *Shigella* invasiveness in epithelial cells through the activation of Rac1.

The physiological role of virA in Shigella invasion

In addition to VirA, *Shigella* secrete other effectors such as IpaA, IpaB and IpaC via the type III secretion system (Sansonetti, 1999; Bourdet-Sicard *et al*., 2000). IpaC may be able to activate Cdc42 and subsequently Rac1, although the mechanism still remains unclear (Tran Van Nhieu *et al*., 1999). Therefore, although it is not clear whether VirA and IpaC share the mutual role of inducing membrane ruffling during bacterial entry or if they act separately, inducing Rac1 activation by means of stimulating distinctive signalling pathways, it seems likely that neither of the activities are sufficient to allow efficient *Shigella* invasion of epithelial cells. Although the *ipaC* mutant of *S.flexneri* has been shown to abolish invasiveness (Ménard *et al*., 1993), it does not necessarily mean that this is its absolute contribution to bacterial internalization, because IpaC can also act as a part of the type III secretion system required for forming a membrane pore with IpaB on the targeted host cells (Blocker *et al*., 1999). Thus the deficiency of IpaC production in *Shigella* would seriously limit the delivery of effector proteins including IpaA, IpaC and VirA into the host cells via the type III secretion system. Under these circumstances, an evaluation of the IpaC (and IpaB) contribution to *Shigella* invasion of epithelial cells is not easy. Nevertheless, to provoke a sufficiently large scale of membrane ruffling to engulf bacteria, additional effector functions including IpaC must be required (Tran Van Nhieu *et al*., 1999) (Figure 9). Although the mechanism underlying the MT destabilization by VirA remains to be elucidated, we believe that VirA-directed membrane ruffling is a unique strategy used by the bacterium to stimulate its own internalization into the mammalian cells.

Materials and methods

Bacterial strains and plasmids

Shigella flexneri (YSH6000), the *virA*::Tn*5* mutant (N1945), the *virA* complement mutant and *mxiA*::Tn*5* mutant (type III secretion-deficient mutant; S325) were described previously (Uchiya *et al*., 1995). A DNA fragment encoding full-length VirA (401 residues) was amplified by PCR using 5′-CGGGATCCATGCAGACATCAAACAT-3′, containing a *Bam*HI site, and 5′-TCCCCCGGGTTAAACATCAGGAGATA-3′. The *Bam*HI–*Eco*RI fragment of the resulting PCR product, encoding VirA residues 1–224, was subcloned into pGEX 4T-1 (Amersham Pharmacia Biotech) to yield pGST-VirA-N224. pKU002(–) was the same as pKU002 (Uchiya *et al*., 1995), but in the opposite direction to the cloned *virA* gene. The *Eco*RI–*Sal*I fragment, encoding VirA residues 224–401, was obtained from pKU002(–) and subcloned into pGST-VirA-N224 or pGEX 4T-1, resulting in pGST-VirA-FL or pGST-VirA-224C, respect-

ively. The *Bam*HI–*Mun*I fragment encoding VirA residues 1–315 was obtained from pGST-VirA-FL and subcloned into pGEX 4T-1, resulting in pGST-VirA-N315. pGST-VirA-224C was digested with *Mun*I and *Not*I before being ligated, to yield pGST-VirA-224/315. After pGST-VirA-224C was digested by *Bsm*I and *Xho*I, the DNA fragment was self-ligated, resulting in pGST-VirA-224/277. The *Bam*HI–*Eco*RI fragment, encoding VirA residues 1–224, was obtained from pGST-VirA-N224 and subcloned into pEGFP-C1 (Clontech), resulting in pVirA-N224. The *Eco*RI–*Sal*I fragment, encoding VirA residues 224–401, was obtained from pKU002 and subcloned into pVirA-N224, resulting in pVirA-FL. The *Bam*HI–*Mun*I fragment, encoding VirA residues 1–315, was obtained from pGST-VirA-FL and subcloned into the *Bgl*II and *Eco*RI sites on pEGFP-C1, resulting in pVirA-N315. Rac1-WT, G12V and T17N were constructed in pEF-BOS (Myc-tagged) (Miki *et al*., 1998).

Cell culture, preparation of GST fusion proteins, microinjection and immunofluorescence microscopy observation

Cell culture, preparation of GST fusion proteins, microinjection and immunofluorescence microscopy were all carried out as described previously (Suzuki *et al*., 1998).

Preparation of purified VirA and tubulin

For use in the immunization of rabbits, the *in vitro* MT destabilization assay and microinjection, the GST fusion proteins were cleaved with thrombin (Sigma-Aldrich) as described previously (Suzuki *et al*., 1998). Purified proteins were dialysed against one of the following buffers: PM buffer [100 mM PIPES–NaOH pH 6.9, 2 mM EGTA, 1 mM $MgSO_4$, 2 mM dithiothreitol (DTT), 1 mM GTP], PM buffer containing 1.3 M glycerol (PM-1.3M buffer) or injection buffer (10 mM Tris–HCl pH 7.5, 150 mM NaCl, 2 mM $MgCl_2$, 0.2 mM β-mercaptoethanol). Bovine brain tubulin was purified as described elsewhere (Williams and Lee, 1982) by two cycles of polymerization and depolymerization (twice-cycled MT proteins), before being stored in PM buffer containing 4 M glycerol at –80°C.

GST pull-down assay

The preparation of bovine brain cytosol fractions was described previously (Miki *et al*., 1994). The fractions were incubated with glutathione–Sepharose-4B beads (Amersham Pharmacia) overnight at 4°C to remove endogenous GST. After centrifugation, the supernatants were incubated overnight with GST–VirA bound to glutathione–Sepharose-4B beads at 4°C. The beads were washed three times with washing buffer A [phosphate-buffered saline (PBS) containing 1% Triton X-100 and 0.15 M NaCl]. The VirA-interacting proteins were then separated by SDS–PAGE, and transferred to polyvinylidene difluoride membranes before being analysed by a Beckman LF3000, or transferred to nitrocellulose membranes and western blotted using an anti-β-tubulin antibody (Sigma). The GST–VirA pull-down assays with cell lysates were carried out as described below. The lysates of HeLa, Swiss 3T3 and COS-7 cells were prepared as described previously (Suzuki *et al*., 1998). The GST fusion proteins bound to the glutathione–Sepharose-4B beads (GST fusion protein beads) were incubated overnight with 1 ml of lysates at 4°C. The samples were then washed three times in washing buffer B [25 mM Tris–HCl pH 7.5, 150 mM NaCl, 1% NP-40, 1 mM Na_3VO_4, 1 mM phenylmethylsulfonyl fluoride (PMSF)], and separated by SDS–PAGE, before being western blotted using a mixture of anti-α-tubulin (Sigma) and anti-β-tubulin antibodies.

In vitro binding assay of taxol-MT and VirA

Taxol-MT was prepared according to the method of Belmont and Mitchison (1996). Briefly, 30 µl of 35 µM tubulin and 3 µl of 35 µM taxol were incubated for 10 min at 37°C, 3 µl of 350 µM taxol was added, and the solution was incubated for another 10 min. The assay was performed as follows: 10 µl of 35 µM taxol-MT and 30 µl of 12 µM purified VirA (test) or 30 µl of PM buffer (control 1) were mixed gently and incubated for 10 min at room temperature. At the same time, 10 µl of PM-4M buffer containing 35 µM taxol and 30 µl of 12 µM purified VirA were also mixed gently and incubated for 10 min at room temperature (control 2). Each mixture was layered onto a 40 µl cushion of 60% glycerol containing 10 µM taxol, and sedimented for 10 min at 100 000 *g* at room temperature. After the centrifugation, the supernatants (total: 80 µl) were added to 20 µl of 5× SDS sample buffer, while the pellets were dissolved into 100 µl of 1× SDS sample buffer. For SDS–PAGE analysis, 9.5 µl of each sample were run on the 10% gel, and the proteins were stained with Coomassie Blue.

In vitro binding assay of tubulin and GST-fusion proteins

For the *in vitro* binding assay, twice-cycled MT proteins were purified further with a P11 phosphocellulose column (Whatman) (Williams and Lee, 1982). Purified tubulin was incubated with the GST fusion protein beads for 1 h at 4°C. The beads were washed five times in PM buffer, and then subjected to SDS–PAGE. The amount of bound protein was determined by western blotting using a mixture of anti-α- and anti-β-tubulin antibodies. Alternatively, to estimate the binding affinity and binding stoichiometry, the protein bound to the beads was subjected to SDS–PAGE without washing. GST beads were used as the control for the estimation to remove the background noise.

In vitro MT destabilization assay

Polymerization of twice-cycled MT proteins was monitored spectrophotometrically (A_{350}) using temperature-controlled cuvettes (37°C) as described previously (Gaskin, 1982; Horwitz *et al*., 1997). To assess the effect of VirA on MT stabilization and destabilization, equal volumes of PM-1.3M buffer alone or PM-1.3M buffer containing VirA were added to the cuvettes either before or after inducing MT polymerization.

X-rhodamine–tubulin assay

X-rhodamine–tubulin was prepared as described by Belmont and Mitchison (1996) and 3.5 mg/ml were polymerized in PM-1.3M buffer at 37°C for 30 min. A 3 µl aliquot of the polymerized X-rhodamine–tubulin was then mixed with 1 µl of 1 mg/ml of VirA or PM buffer (control) by gently pipetting up and down three times. After the sample was diluted into 100 µl of PM-1.3M buffer, 4 µl was placed on a poly-L-lysine-coated glass slide, and covered with an 18 × 24 mm coverslip. The shape of the MTs was observed by confocal microscopy (Micro Radiance Plus; Bio-Rad) at 0, 10, 20 and 30 min after setting them on the microscope stage. All slides were exposed for the same duration and to the same intensity of fluorescent light. The means and SEM were calculated from the results of three independent experiments. At time 0, the length of 20 MTs was measured, and the changes in each MT were monitored for 30 min.

Transfection and immunostaining

For overexpression of GFP fusion proteins in COS-7 cells, 2×10^6 COS-7 cells were mixed with each of the purified plasmids (pEGFP-C1, 5 µg; pVirA-N224, 10 µg; pVirA-N315, 15 µg; and pVirA-FL, 30 µg) before being transfected by electroporation. The cells were reseeded on glass coverslips and cultured for 18 h. After this time, ~10% of the cells expressed GFP or GFP fusion proteins. For co-expression of GFP–VirA and Rac-T17N in COS-7 cells, both purified plasmids (pVirA-FL, 30 µg; Rac-T17N expression plasmid, 10 µg) were transfected into COS-7 cells as described above. After an 18 h culture, ~5% of the cells expressed both GFP–VirA and myc-Rac. For overexpression of GFP fusion proteins in HeLa cells, 2×10^6 HeLa cells were mixed with pEGFP-C1 (0.25 µg) and pVirA-FL (1 µg), before being transfected by FuGENE 6 (Roche). The cells were cultured for 18 h and, after this time, ~5% of the cells expressed GFP or GFP–VirA. The samples were washed with PBS and then fixed in PBS containing 4% paraformaldehyde for 20 min. After further washing with PBS, the samples were incubated with 50 mM NH_4Cl in PBS for 10 min. The cells were then permeabilized by a 20 min incubation with 0.2% Triton X-100 in PBS, and blocked with 2% bovine serum albumin (BSA) in Tris-buffered saline (TBS) for 30 min. The actin and MTs were visualized by staining with either rhodamine-labelled phalloidin (Molecular Probes) or a mixture of anti-α-tubulin and anti-β-tubulin antibodies followed by Cy5-anti-mouse IgG, respectively. The transfected cells were identified by visualizing the GFP.

Rac1 activity assay

A DNA fragment encoding Pak-1 residues 31–100 including the Rac1-binding domain (PBD; the Pak-binding domain; Burbelo *et al*., 1995) was amplified by PCR using 5′-CGGGATCCAACCATGGTTCTAA-ACCTCTGCCT-3′ and 5′-CGGAATTCTGGCATTCCCGTAAACTC-CCCTGT-3′, containing a *Bam*HI site and an *Eco*RI site in the 5′ tail, respectively. The PCR product was subcloned into pGEX 4T-1, resulting in pGST-PBD. The PBD domain of Pak-1 fused with GST (GST–PBD) was first checked for its capacity to bind to the active form of Rac1. A total of 2×10^6 COS-7 cells were mixed with Myc-tagged Rac-WT, G12V or T17N expression plasmids (10 µg), and transfected by electroporation. The cells were reseeded and cultured for 24 h. At this time, ~20% of the cells expressed Myc-Rac. The lysates were prepared as described before (Waterman-Storer *et al*., 1999), and then incubated with GST–PBD (40 µg) bound to glutathione–Sepharose-4B beads (GST–PBD beads) at 4°C overnight. The beads were washed three times in washing

buffer B before being subjected to SDS–PAGE, and western blotting using an anti-Rac1 antibody (Upstate Biotechnology). GST–PBD could only recognize the active form of Rac1 (V12Rac) and not the wild-type or negative form of Rac1 (N17Rac), proving the validity of using GST–PBD beads (data not shown). To examine the level of Rac1 activity in infected cells, a total of 5×10^6 HeLa cells were infected with wild-type, *virA* mutant, the *virA* complement mutant or a *mxiA* mutant. After incubating at 37°C for 12 min, the cells were lysed in 1 ml of assay buffer. The lysates were subsequently incubated with GST–PBD (40 μg) beads at 4°C overnight. The beads were then washed, and the eluted proteins separated by SDS–PAGE before being analyzed by western blotting as described above.

Other biological assays

Infection of cultured cells was carried out as described previously (Suzuki *et al*., 1998). After a 5–15 min incubation at 37°C, the cells were washed, fixed, permeabilized and blocked. The actin and MTs were visualized by staining with either rhodamine-labelled phalloidin, or a mixture of anti-α-tubulin and anti-β-tubulin antibodies followed by Cy5-anti mouse IgG antibody, respectively. VirA was visualized by staining with an anti-VirA antibody followed by an Alexa 488-labelled anti-rabbit IgG antibody. The number of membrane ruffles per infected cell was determined by counting the rhodamine–phalloidin-labelled membrane ruffles in 15 fields for each experiment. The 'nocodazole washing out invasion assay' was carried out as follows: the MT-destabilizing drug nocodazole (Sigma-Aldrich) was used for inducing MT growth in HeLa cells (Waterman-Storer *et al*., 1999). The cells were pre-treated with 10 μM nocodazole. Subsequently, the drug was washed out by changing the medium, and the cells incubated for a further 10 min at 37°C. The assays for measuring the number of membrane ruffles and numbers of internalized bacteria were carried out as described above. The means and SEM were calculated from the results of three independent experiments.

Acknowledgements

We are grateful to the reviewers for their valuable suggestions. We thank Takahito Toyotome, Hiroki Iwai, Ichiro Tatsuno and Toru Tobe for helpful discussions, and Shinobu Imajoh-Ohmi and Takashi Nonaka for helpful advice. This work was supported by the Research for the Future Program of the Japan Society for the Promotion of Science, Grant-in-aid for Scientific Research from the Japanese Ministry of Education, Science, Sports and Culture, and PRESTO, Japan Science and Technology Corporation (JST).

References

Belmont,L.D. and Mitchison,T.J. (1996) Identification of a protein that interacts with tubulin dimers and increases the catastrophe rate of microtubules. *Cell*, **84**, 623–631.

Blocker,A., Gounon,P., Larquet,E., Niebuhr,K., Cabiaux,V., Parsot,C. and Sansonetti,P. (1999) The tripartite type III secretion of *Shigella flexneri* inserts IpaB and IpaC into host membranes. *J. Cell Biol.*, **147**, 683–693.

Bourdet-Sicard,R., Rüdiger,M., Jockusch,B.M., Gounon,P., Sansonetti, P.J. and Tran Van Nhieu,G. (1999) Binding of the *Shigella* protein IpaA to vinculin induces F-actin depolymerization. *EMBO J.*, **18**, 5853–5862.

Bourdet-Sicard,R., Egile,C., Sansonetti,P.J. and Tran Van Nhieu,G. (2000) Diversion of cytoskeletal processes by *Shigella* during invasion of epithelial cells. *Microbes Infect.*, **2**, 813–819.

Burbelo,P.D., Drechsel,D. and Hall,A. (1995) A conserved binding motif defines numerous candidate target proteins for both Cdc42 and Rac GTPases. *J. Biol. Chem.*, **270**, 29071–29074.

Cassimeris,L. (2002) The oncoprotein 18/stathmin family of microtubule destabilizers. *Curr. Opin. Cell Biol.*, **14**, 18–24.

Cossart,P. and Lecuit,M. (1998) Interactions of *Listeria monocytogenes* with mammalian cells during entry and actin-based movement: bacterial factors, cellular ligands and signaling. *EMBO J.*, **17**, 3797–3806.

Demers,B., Sansonetti,P.J. and Parsot,C. (1998) Induction of type III secretion in *Shigella flexneri* is associated with differential control of transcription of genes encoding secreted proteins. *EMBO J.*, **17**, 2894–2903.

Desai,A. and Mitchison,T.J. (1997) Microtubule polymerization dynamics. *Annu. Rev. Cell. Dev. Biol.*, **13**, 83–117.

Desai,A., Verma,S., Mitchison,T.J. and Walczak,C.E. (1999) Kin I kinesins are microtubule-destabilizing enzymes. *Cell*, **96**, 69–78.

Drewes,G., Ebneth,A., Preuss,U., Mandelkow,E.-M. and Mandelkow,E. (1997) MARK, a novel family of protein kinases that phosphorylate microtubule-associated proteins and trigger microtubule disruption. *Cell*, **89**, 297–308.

Finlay,B.B. and Falkow,S. (1997) Common themes in microbial pathogenicity revisited. *Microbiol. Mol. Biol. Rev.*, **61**, 136–169.

Francis,C.L., Ryan,T.A., Jones,B.D., Smith S.J. and Falkow,S. (1993) Ruffles induced by *Salmonella* and other stimuli direct macropinocytosis of bacteria. *Nature*, **364**, 639–642.

Galán,J.E. and Zhou,D. (2000) Striking a balance: modulation of the actin cytoskeleton by *Salmonella*. *Proc. Natl Acad. Sci. USA*, **97**, 8754–8761.

Gaskin,F. (1982) Techniques for the study of microtubule assembly *in vitro*. *Methods Enzymol.*, **85**, 433–439.

Gavet,O., Ozon,S., Manceau,V., Lawler,S., Curmi,P. and Sobel,A. (1998) The stathmin phosphoprotein family: intracellular localization and effects on the microtubule network. *J. Cell Sci.*, **111**, 3333–3346.

Horwitz,A.R. and Parsons,J.T. (1999) Cell migration—movin'on. *Science*, **286**, 1102–1103.

Horwitz,S.B., Shen,H.-J., He,L., Dittmar,P., Neef,R., Chen,J. and Schubart,U.K. (1997) The microtubule-destabilizing activity of metablastin (p19) is controlled by phosphorylation. *J. Biol. Chem.*, **272**, 8129–8132.

Ireton,K. and Cossart,P. (1998) Interaction of invasive bacteria with host signaling pathways. *Curr. Opin. Cell Biol.*, **10**, 276–283.

Isberg,R.R. (1991) Discrimination between intracellular uptake and surface adhesion of bacterial pathogens. *Science*, **252**, 934–938.

Isberg,R.R. and Tran Van Nhieu,G. (1994) Binding and internalization of microorganisms by integrin receptors. *Trends Microbiol.*, **2**, 10–14.

Kuhn,M. (1998) The microtubule depolymerizing drugs nocodazole and colchicine inhibit the uptake of *Listeria monocytogenes* by P388D1 macrophages. *FEMS Microbiol. Lett.*, **160**, 87–90.

Kuwae,A., Yoshida,S., Tamano,K., Mimuro,H., Suzuki,T. and Sasakawa,C. (2001) *Shigella* invasion of macrophage requires the insertion of IpaC into the host plasma membrane. *J. Biol. Chem.*, **276**, 32230–32239.

McNally,F.J. and Vale,R.D. (1993) Identification of katanin, an ATPase that severs and disassembles stable microtubules. *Cell*, **75**, 419–429.

Ménard,R., Sansonetti,P.J. and Parsot,C. (1993) Nonpolar mutagenesis of the *ipa* genes defines IpaB, IpaC and IpaD as effectors of *Shigella fexneri* entry into epithelial cells. *J. Bacteriol*., **175**, 5899–5906.

Meyer,D.H., Rose,J.E., Lippmann,J.E. and Fives-Taylor,P.M. (1999) Microtubules are associated with intracellular movement and spread of the periodontopathogen *Actinobacillus actinomycetemcomitans*. *Infect. Immun.*, **67**, 6518–6525.

Mikhailov,A. and Gundersen,G.G. (1998) Relationship between microtubule dynamics and lamellipodium formation revealed by direct imaging of microtubules in cells treated with nocodazole or taxol. *Cell Motil. Cytoskel.*, **41**, 325–340.

Miki,H., Miura,K., Matuoka,K., Nakata,T., Hirokawa,N., Orita,S., Kaibuchi,K., Takai,Y. and Takenawa,T. (1994) Association of Ash/Grb-2 with dynamin through the Src homology 3 domain. *J. Biol. Chem.*, **269**, 5489–5492.

Miki,H., Suetsugu,S. and Takenawa,T. (1998) WAVE, a novel WASP-family protein involved in actin reorganization induced by Rac. *EMBO J.*, **17**, 6932–6941.

Mounier,J., Laurent,V., Hall,A., Fort,P., Carlier,M.-F., Sansonetti,P.J. and Egile,C. (1999) Rho family GTPases control entry of *Shigella flexneri* into epithelial cells but not intracellular motility. *J. Cell Sci.*, **112**, 2069–2080.

Oelschlaeger,T.A., Guerry,P. and Kopecko,D.J. (1993) Unusual microtubule-dependent endocytosis mechanisms triggered by *Campylobacter jejuni* and *Citrobacter freundii*. *Proc. Natl Acad. Sci. USA*, **90**, 6884–6888.

Ookata,K. *et al*. (1995) Cyclin B interaction with microtubule-associated protein 4 (MAP4) targets $p34^{cdc2}$ kinase to microtubules and is a potential regulator of M-phase microtubule dynamics. *J. Cell Biol.*, **128**, 849–862.

Ren,X.-D., Kiosses,W.B. and Schwartz,M.A. (1999) Regulation of the small GTP-binding protein Rho by cell adhesion and the cytoskeleton. *EMBO J.*, **18**, 578–585.

Sansonetti,P.J. (1999) *Shigella* plays dangerous games. *ASM News*, **65**, 611–617.

Shelden,E. and Wadsworth,P. (1993) Observation and quantification of

individual microtubule behavior *in vivo*: microtubule dynamics are cell-type specific. *J. Cell Biol.*, **120**, 935–945.
Suzuki,T., Miki,H., Takenawa,T. and Sasakawa,C. (1998) Neural Wiskott–Aldrich syndrome protein is implicated in the actin-based motility of *Shigella flexneri*. *EMBO J.*, **17**, 2767–2776.
Tran Van Nhieu,G., Ben-Ze'ev,A. and Sansonetti,P.J. (1997) Modulation of bacterial entry into epithelial cells by association between vinculin and the *Shigella* IpaA invasin. *EMBO J.*, **16**, 2717–2729.
Tran Van Nhieu,G., Caron,E., Hall,A. and Sansonetti,P.J. (1999) IpaC induces actin polymerization and filopodia formation during *Shigella* entry into epithelial cells. *EMBO J.*, **18**, 3249–3262.
Uchiya,K., Tobe,T., Komatsu,K., Suzuki,T., Watarai,M., Fukuda,I., Yoshikawa,M. and Sasakawa,C. (1995) Identification of a novel virulence gene, *virA*, on the large plasmid of *Shigella*, involved in invasion and intercellular spreading. *Mol. Microbiol.*, **17**, 241–250.
Wadsworth,P. and Bottaro,D.P. (1996) Microtubule dynamic turnover is suppressed during polarization and stimulated in hepatocyte growth factor scattered Madin–Darby canine kidney epithelial cells. *Cell Motil. Cytoskel.*, **35**, 225–236.
Watarai,M., Kamata,Y., Kozaki,S. and Sasakawa,C. (1997) rho, a small GTP-binding protein, is essential for *Shigella* invasion of epithelial cells. *J. Exp. Med.*, **185**, 281–292.
Waterman-Storer,C.M. and Salmon,E.D. (1997) Actomyosin-based retrograde flow of microtubules in the lamella of migrating epithelial cells influences microtubule dynamic instability and turnover and is associated with microtubule breakage and treadmilling. *J. Cell Biol.*, **139**, 417–434.
Waterman-Storer,C.M. and Salmon,E.D. (1999) Positive feedback interactions between microtubule and actin dynamics during cell motility. *Curr. Opin. Cell Biol.*, **11**, 61–67.
Waterman-Storer,C.M., Worthylake,R.A., Liu,B.P., Burridge,K. and Salmon,E.D. (1999) Microtubule growth activates Rac1 to promote lamellipodial protrusion in fibroblasts. *Nature Cell Biol.*, **1**, 45–50.
Williams,R.C.Jr and Lee,J.C. (1982) Preparation of tubulin from brain. *Methods Enzymol.*, **85**, 376–385.
Wittmann,T. and Waterman-Storer,C.M. (2001) Cell motility: can Rho GTPases and microtubules point the way? *J. Cell Sci.*, **114**, 3795–3803.

Received October 1, 2001; revised April 4, 2002;
accepted April 30, 2002